Localized dynamic kinetic-energy-based models for stochastic coherent adaptive large eddy simulation

Giuliano De Stefano,[1,a)] Oleg V. Vasilyev,[2,b)] and Daniel E. Goldstein[3]
[1]*Dipartimento di Ingegneria Aerospaziale e Meccanica, Seconda Università di Napoli, I 81031 Aversa, Italy*
[2]*Department of Mechanical Engineering, University of Colorado at Boulder, Boulder, Colorado 80309, USA*
[3]*Northwest Research Associates, Inc., CORA Division, Boulder, Colorado 80301, USA*

(Received 19 July 2007; accepted 6 February 2008; published online 8 April 2008)

Stochastic coherent adaptive large eddy simulation (SCALES) is an extension of the large eddy simulation approach in which a wavelet filter-based dynamic grid adaptation strategy is employed to solve for the most "energetic" coherent structures in a turbulent field while modeling the effect of the less energetic background flow. In order to take full advantage of the ability of the method in simulating complex flows, the use of localized subgrid-scale models is required. In this paper, new local dynamic one-equation subgrid-scale models based on both eddy-viscosity and non-eddy-viscosity assumptions are proposed for SCALES. The models involve the definition of an additional field variable that represents the kinetic energy associated with the unresolved motions. This way, the energy transfer between resolved and residual flow structures is explicitly taken into account by the modeling procedure without an equilibrium assumption, as in the classical Smagorinsky approach. The wavelet-filtered incompressible Navier–Stokes equations for the velocity field, along with the additional evolution equation for the subgrid-scale kinetic energy variable, are numerically solved by means of the dynamically adaptive wavelet collocation solver. The proposed models are tested for freely decaying homogeneous turbulence at $\mathrm{Re}_\lambda = 72$. It is shown that the SCALES results, obtained with less than 0.5% of the total nonadaptive computational nodes, closely match reference data from direct numerical simulation. In contrast to classical large eddy simulation, where the energetic small scales are poorly simulated, the agreement holds not only in terms of global statistical quantities but also in terms of spectral distribution of energy and, more importantly, enstrophy all the way down to the dissipative scales. © *2008 American Institute of Physics*. [DOI: 10.1063/1.2896283]

I. INTRODUCTION

In the large eddy simulation (LES) approach to numerical simulation of turbulence, only the large-scale motions are solved for while modeling the effect of the unresolved subgrid-scale (SGS) eddies. Though there has been considerable progress in the development of the methodology since the pioneering works on the subject (e.g., Refs. 1 and 2), mostly due to the introduction of the dynamic modeling procedure,[3] the LES method is not yet considered a predictive tool for engineering applications.

Apart from the computational cost that becomes unaffordable for high Reynolds-number flows, some conceptual aspects of the LES methodology need to be improved in order to make it more feasible. In particular, following Ref. 4, one can recognize that most current LES methods are not "complete," where the governing equations are actually not free from flow-dependent *ad hoc* prescriptions. In particular, the formal scale separation is typically obtained via low-pass implicit grid filtering, so that the extent of the resolved scale range (i.e., the turbulence resolution) directly links to the adopted numerical resolution. As generally conducted, a LES calculation involves a prescribed numerical grid with given (possibly nonuniform) grid spacing, where the numerical mesh is chosen in a somewhat subjective manner to ensure the adequate resolution for the different desired flow realizations.

The above mentioned shortcomings have been recently addressed by the introduction of a novel approach to LES, referred to as the stochastic coherent adaptive large eddy simulation (SCALES).[5] The basic idea is to solve only for the most energetic coherent eddies in a turbulent field while modeling the effect of the less energetic (unresolved) motions. A wavelet thresholding filter is employed to perform the dynamic grid adaptation that identifies and tracks the structures of significant energy in the flow. Such an adaptive-gridding strategy makes the method more "complete" with respect to classical LES, even though it is still not fully free from subjective specifications.

Similarly to any LES approach, the SCALES method is supplied with a closure model for the residual stress term that is mainly required to mimic the energy transfer between the resolved and the unresolved motions. In fact, the SGS dissipation has been shown to be dominated by a minority of subgrid-scale coherent eddies, while the majority of incoher-

[a)]Electronic mail: giuliano.destefano@unina2.it. URL: http://www.diam.unina2.it.
[b)]Electronic mail: Oleg.Vasilyev@Colorado.edu. URL: http://multiscalemodeling.colorado.edu/vasilyev.

ent SGS motions negligibly contribute to the total energy transfer (e.g., Refs. 5 and 6). For this reason, as usual in most LES formulations, in this work only the effect of coherent SGS motions is approximated through a deterministic model, while the development of a stochastic model to capture the effect of the incoherent unresolved motions may be the subject of a future work.

The first step toward the construction of SGS models for SCALES was successfully undertaken in Ref. 7, where a dynamic Smagorinsky model, based on the extension of the classical Germano procedure redefined in terms of wavelet thresholding filters, was developed. The main drawback of this formulation was the use of a global (spatially nonvariable) model coefficient resulting from the volume-averaging operation performed to stabilize the numerical solution. This unnecessarily limited the approach to flows with at least one homogeneous direction, thus excluding the treatment of complex geometry flows. This is unfortunate since the dynamic adaptability of the method is ideally suited to inhomogeneous flow simulation, for which the SGS model coefficient should be, instead, a function of position. More sophisticated localized models must therefore be developed to make the SCALES approach a viable tool for engineering applications. For instance, in a more recent study, a local dynamic model based on the Lagrangian pathline averaging approach has been proposed (e.g., Ref. 8).

In the present work, the locality of the model is achieved by explicitly taking into account the energy transfer between resolved and residual motions. This appears as a natural choice in the SCALES framework since the desired turbulence resolution directly links to the resolved kinetic energy content. To ensure the energy budget, an additional model transport equation for the unknown SGS kinetic energy is numerically solved along with the momentum equation. Such a modeling procedure allows for the significant energy backscatter that exists from unresolved motions toward the coherent resolved eddies (however, the net energy transfer is in the opposite sense) to be simulated. This way, an automatic local feedback mechanism is provided that stabilizes the solution without the need of any averaging procedure, making it possible to simulate nonhomogeneous flows.

The paper is organized as follows. The SCALES methodology for the numerical solution of turbulent flows is briefly reviewed in Sec. II. The general features of the new localized modeling procedure involving the SGS kinetic energy definition, along with the pertinent transport equation, are discussed in Sec. III. Different local dynamic kinetic-energy-based eddy-viscosity models, exploiting either Bardina or Germano approximations, are proposed in Sec. IV, while the non-eddy-viscosity "dynamic structure" model (DSM) for SCALES is introduced in Sec. V. The results of numerical experiments carried out for freely decaying isotropic turbulence, as an example of statistically unsteady flows, are discussed in Sec. VI. Finally, in Sec. VII, some concluding remarks and perspectives are given.

II. SCALES METHOD

In this section, the SCALES method is briefly reviewed. After defining the wavelet thresholding filtering procedure, the SCALES governing equations for turbulent incompressible flows are introduced, along with the method for the numerical solution.

A. Wavelet thresholding filter

The wavelet thresholding filter is a key component of the SCALES methodology. The instantaneous velocity field $u_i(\mathbf{x})$ can be represented in terms of wavelet basis functions as

$$u_i(\mathbf{x}) = \sum_{\mathbf{l}\in\mathcal{L}^0} c_{\mathbf{l}}^0 \phi_{\mathbf{l}}^0(\mathbf{x}) + \sum_{j=0}^{+\infty} \sum_{\mu=1}^{2^n-1} \sum_{\mathbf{k}\in\mathcal{K}^{\mu,j}} d_{\mathbf{k}}^{\mu,j} \psi_{\mathbf{k}}^{\mu,j}(\mathbf{x}), \tag{1}$$

where $\phi_{\mathbf{l}}^0$ and $\psi_{\mathbf{k}}^{\mu,j}$ are n-dimensional scaling functions and wavelets of different families and levels of resolution (indexed with μ and j, respectively). One may think of the above wavelet decomposition as a multilevel or multiresolution representation of the pointwise function u_i, where each level of resolution j (except the coarsest one) consists of a family of wavelets $\psi_{\mathbf{k}}^{\mu,j}$ having the same scale but located at different positions. The scaling function coefficients $c_{\mathbf{l}}^0$ represent the averaged values of the velocity field, whereas the wavelet coefficients $d_{\mathbf{k}}^{\mu,j}$ represent the details of the field at different scales. Intuitively, one can think of the coefficient $d_{\mathbf{k}}^{\mu,j}$ in the wavelet decomposition (1) as being negligible unless u_i shows significant variation on the j level of resolution in the immediate vicinity of the position associated with the wavelet $\psi_{\mathbf{k}}^{\mu,j}$. Once the physical domain is discretized by means of a numerical grid, a one-to-one correspondence between grid points and wavelet coefficients is introduced.

Wavelet filtering is performed in the wavelet space through wavelet coefficient thresholding. Namely, the wavelet filtered velocity is defined as follows:

$$\overline{u}_i^{>\epsilon}(\mathbf{x}) = \sum_{\mathbf{l}\in\mathcal{L}^0} c_{\mathbf{l}}^0 \phi_{\mathbf{l}}^0(\mathbf{x}) + \sum_{j=0}^{j_{\max}} \sum_{\mu=1}^{2^n-1} \sum_{\substack{\mathbf{k}\in\mathcal{K}^{\mu,j} \\ |d_{\mathbf{k}}^{\mu,j}|>\epsilon U_i}} d_{\mathbf{k}}^{\mu,j} \psi_{\mathbf{k}}^{\mu,j}(\mathbf{x}), \tag{2}$$

where $\epsilon > 0$ stands for the prescribed nondimensional relative thresholding level and U_i is the absolute velocity scale along the ith direction. For homogeneous turbulence, the velocity scale must be considered independent of direction and can be fixed, for instance, as the L_2 norm of the velocity vector field. Since the actual absolute threshold derives from the time-dependent velocity field, the wavelet thresholding filter must be thought of as a nonlinear filter that depends on each flow realization. However, the filtering procedure is uniquely determined by fixing the thresholding level ϵ. The wavelet filtered velocity (2) corresponds by definition to the most energetic flow eddies and is often referred to as the "coherent" velocity in the literature, e.g., Ref. 9.

The major strength of wavelet filtering is in the ability to "compress" the solution. For turbulent fields that typically contain isolated high-energy structures on a low-energy

background flow, most wavelet coefficients are, in fact, negligible. Thus, a good approximation to the unfiltered field can be obtained even after discarding a large number of wavelets with small coefficients. The grid compression, defined as the ratio between the number of discarded wavelets and the total number of wavelets (that corresponds to the number of available grid points), is a fundamental parameter in the present methodology. For example, by applying a similar wavelet decomposition to a given isotropic turbulent field at $\mathrm{Re}_\lambda = 168$, it has been demonstrated in Ref. 10 that one is able to capture as much as 99.1% of the kinetic energy content of the flow by retaining only 2.9% of the wavelet coefficients.

B. Governing equations

The SCALES equations, which describe the space-time evolution of the most energetic coherent eddies in a turbulent flow, can be formally obtained by applying the wavelet thresholding filter (2) to the Navier–Stokes equations. Disregarding the commutation error between wavelet filtering and differentiation, the SCALES governing equations for incompressible flows are written as the following filtered continuity and momentum equations:

$$\frac{\partial \overline{u}_i^{>\epsilon}}{\partial x_i} = 0, \tag{3}$$

$$\frac{\partial \overline{u}_i^{>\epsilon}}{\partial t} + \overline{u}_j^{>\epsilon}\frac{\partial \overline{u}_i^{>\epsilon}}{\partial x_j} = -\frac{1}{\rho}\frac{\partial \overline{p}^{>\epsilon}}{\partial x_i} + \nu\frac{\partial^2 \overline{u}_i^{>\epsilon}}{\partial x_j \partial x_j} - \frac{\partial \tau_{ij}}{\partial x_j}, \tag{4}$$

where ρ and ν are the constant density and kinematic viscosity of the fluid, while p stands for the pressure field. Like in the classical LES formulation, as a result of the filtering process, the unresolved quantities

$$\tau_{ij} = \overline{u_i u_j}^{>\epsilon} - \overline{u}_i^{>\epsilon}\overline{u}_j^{>\epsilon}, \tag{5}$$

commonly referred to as SGS stresses, are introduced. In this context, they can be thought of representing the effect of unresolved less energetic eddies on the dynamics of the resolved energetic coherent vortices. In order to close the filtered equation (4), a SGS model is required to express the unknown stresses (5) as a given function of the resolved velocity field. In practice, the isotropic part of the SGS stress tensor is usually incorporated by a modified filtered pressure variable, so that only the deviatoric part, hereafter noted with a star, $\tau_{ij}^* = \tau_{ij} - \frac{1}{3}\tau_{kk}\delta_{ij}$, is actually modeled. Henceforth, the filtered momentum equation can be rewritten as

$$\frac{\partial \overline{u}_i^{>\epsilon}}{\partial t} + \overline{u}_j^{>\epsilon}\frac{\partial \overline{u}_i^{>\epsilon}}{\partial x_j} = -\frac{\partial \overline{P}^{>\epsilon}}{\partial x_i} + \nu\frac{\partial^2 \overline{u}_i^{>\epsilon}}{\partial x_j \partial x_j} - \frac{\partial \tau_{ij}^*}{\partial x_j}, \tag{6}$$

where $\overline{P}^{>\epsilon} = \overline{p}^{>\epsilon}/\rho + \frac{1}{3}\tau_{kk}$.

It is worth stressing that for a suitably low value of the wavelet thresholding level ϵ, the resulting SGS field closely resembles Gaussian white noise and no modeling procedure is required in practice to recover low order direct numerical simulations (DNS) statistics. This approach, referred to as the coherent vortex simulation (CVS), which was originally introduced in Ref. 9, has been recently successfully applied to isotropic turbulence simulation in Ref. 7.

Before reviewing the numerical implementation of the SCALES methodology, let us discuss in more detail the wavelet filtering of the Navier–Stokes equations, in terms of both practical application and formal interpretation. Due to the one-to-one correspondence between wavelets and grid points, filtering each scalar field variable with the corresponding absolute scale would lead to numerical complications since each variable should be solved on a different numerical grid. In the present study, in order to avoid this difficulty, the coupled wavelet thresholding strategy is adopted. Namely, after constructing the mask of significant wavelet coefficients for each primary variable, the union of these masks results in a global thresholding mask that is used as a common mask for filtering all the variables. Moreover, according to the definition (2), the absolute filtering threshold should be theoretically based on the values of the unfiltered variable, whereas, in a real SCALES calculation, the filtering procedure is actually based on the values of the resolved filtered variable. However, as demonstrated in Ref. 7, this approximation is fully acceptable. For instance, regarding the velocity scale, in the homogeneous case, one can use $U_i = \langle 2k_{\mathrm{res}}\rangle^{1/2}$, where the angular brackets denote volume averaging and

$$k_{\mathrm{res}} = \tfrac{1}{2}\overline{u}_j^{>\epsilon}\overline{u}_j^{>\epsilon} \tag{7}$$

stands for the resolved kinetic energy.

As to wavelet filtering interpretation, one can view the wavelet thresholding procedure as a local spatially variable time-dependent low-pass filter that removes the high wavenumber components of the flow field. The local characteristic filter width, say, $\Delta(\boldsymbol{x},t)$, which is implicitly defined by the thresholding procedure and can be extracted from the global mask during the simulation, is to be interpreted as the actual turbulence-resolution length scale.[4] In fact, it is a measure of the local numerical resolution with the minimum allowable characteristic width corresponding to the highest level $j_{\max}$ in Eq. (2). The smaller the value of ϵ, the smaller the length scale Δ and the greater the fraction of resolved kinetic energy in any local region of the domain. In the limit of vanishing ϵ, the wavelet-based DNS solution is obtained over the whole domain. Such an interpretation of the wavelet thresholding filter highlights the similarity between the SCALES and the classical LES approaches. However, the wavelet filter is distinctively different from the usual filters adopted in LES, primarily because it changes in time following the flow evolution. This results in using a self-adaptive computational grid that tracks the areas of significant energy in the physical space during the simulation.

C. Numerical implementation

The SCALES methodology is numerically implemented by means of the adaptive wavelet collocation method (AWCM), e.g., Ref. 11. The wavelet collocation method employs wavelet compression as an integral part of the numerical algorithm such that the solution is obtained with the minimum number of grid points for a given accuracy.

Briefly, the AWCM method is an adaptive variable order finite-difference method for solving partial differential equa-

tions with localized structures that change their location and scale. As the computational grid automatically adapts to the solution, in both position and scale, one does not have to know *a priori* where the regions of high gradients or localized structures in the flow exist. Moreover, the method has a computational complexity $O(N)$, where N is the number of wavelets retained in the calculation, i.e., those wavelets with a significant coefficient for at least one primary variable (given the coupled wavelet thresholding strategy), plus nearest neighbors.

As to time integration, a multistep pressure correction method[12] is employed for the integration of Eq. (4) with the continuity constraint (3). The resulting Poisson equation is solved with an AWCM.[13]

III. KINETIC-ENERGY-BASED MODELING

In order to take full advantage of the SCALES methodology for simulating complex turbulent flows, the development of localized closure models appears necessary. For this purpose, a modeling mechanism that takes into account the local kinetic energy transfer back and forth between resolved and unresolved eddies can be exploited. In fact, as the closure model is mainly required to provide the right rate of energy dissipation from the resolved field, the model coefficient can be calibrated on the energy level of the residual motions. It has been demonstrated in Ref. 14 that energy-based localized models for LES can be successfully constructed by incorporating a transport model equation for the residual kinetic energy. Moreover, the use of the kinetic energy variable appears as a natural choice in the present context, given the main feature of the SCALES approach, which consists in solving for the significant part of the energy content of the flow field while modeling the effect of the less energetic background flow. In this work, the use of both local eddy-viscosity and non-eddy-viscosity kinetic-energy-based models in the context of SCALES is explored.

In order to address some issues about the local energy transfer between resolved and residual motions, let us first consider the balance equation for the resolved kinetic energy, i.e., according to Eq. (6),

$$\frac{\partial k_{\mathrm{res}}}{\partial t}+\overline{u}_j^{>\epsilon}\frac{\partial k_{\mathrm{res}}}{\partial x_j}=-\frac{\partial}{\partial x_i}[\overline{u}_j^{>\epsilon}(\tau_{ij}^*+\overline{P}^{>\epsilon}\delta_{ij})]+\nu\frac{\partial^2 k_{\mathrm{res}}}{\partial x_j\partial x_j}-\epsilon_{\mathrm{res}}-\Pi, \tag{8}$$

where $\epsilon_{\mathrm{res}}=\nu(\partial\overline{u}_i^{>\epsilon}/\partial x_j)(\partial\overline{u}_i^{>\epsilon}/\partial x_j)$ stands for the rate of resolved viscous dissipation and $\Pi=-\tau_{ij}^*\overline{S}_{ij}^{>\epsilon}$ represents the rate at which energy is transferred to unresolved residual motions. As to resolved viscous dissipation, it is worth pointing out that ϵ_{res} is not negligible for SCALES, in contrast to what typically happens for classical LES. This is mostly due to the adaptive nature of the SCALES approach, which results in the presence of significant energy at small scales, as demonstrated in Sec. VI. Note also that the local energy transfer Π can show both signs, even though energy is globally transferred from resolved to residual motions, e.g., $\langle\Pi\rangle>0$ for isotropic turbulence. For this reason, Π is commonly referred to as the SGS dissipation.

The SGS kinetic energy, say, k_{SGS}, is formally defined as the difference between the wavelet filtered energy and the kinetic energy of the filtered velocity field, k_{res}, that is,

$$k_{\mathrm{SGS}}=\tfrac{1}{2}(\overline{u_i u_i}^{>\epsilon}-\overline{u}_i^{>\epsilon}\overline{u}_i^{>\epsilon}). \tag{9}$$

The above energy variable is simply related to the trace of the SGS stress tensor, where $k_{\mathrm{SGS}}=\frac{1}{2}\tau_{ii}$. Note that the adopted terminology is in some way inappropriate as this quantity does not stand for the kinetic energy associated with the SGS motions, which is $\frac{1}{2}\overline{u_i' u_i'}^{>\epsilon}$, where $u_i'=u_i-\overline{u}_i^{>\epsilon}$ is the residual velocity field. The evolution of k_{SGS} can be modeled by means of the following transport equation (e.g., Ref. 14):

$$\frac{\partial k_{\mathrm{SGS}}}{\partial t}+\overline{u}_j^{>\epsilon}\frac{\partial k_{\mathrm{SGS}}}{\partial x_j}=\nu\frac{\partial^2 k_{\mathrm{SGS}}}{\partial x_j\partial x_j}-\epsilon_{\mathrm{SGS}}+\Pi, \tag{10}$$

where ϵ_{SGS} stands for the viscous dissipation rate of the SGS kinetic energy, that is, the unclosed term

$$\epsilon_{\mathrm{SGS}}=\nu\left(\overline{\frac{\partial u_i}{\partial x_j}\frac{\partial u_i}{\partial x_j}}^{>\epsilon}-\frac{\partial\overline{u}_i^{>\epsilon}}{\partial x_j}\frac{\partial\overline{u}_i^{>\epsilon}}{\partial x_j}\right). \tag{11}$$

In order to close the energy equation (10), a further model for the SGS viscous dissipation ϵ_{SGS} must be introduced, as discussed in the following section.

The SGS energy production Π takes a fundamental role in modeling procedures based on the kinetic energy variable. As it contributes with different signs to both resolved (8) and SGS (10) energy balances, it can be exploited to develop a built-in feedback mechanism that automatically stabilizes the numerical solution. This way, no averaging procedure is needed and the full locality of the model is achieved. Namely, one can assume the SGS dissipation to be a monotonic increasing function of k_{SGS} so that, for example, if there is energy backscatter from unresolved to resolved motions (i.e., $\Pi<0$), the resolved kinetic energy locally increases while the residual one decreases, but the SGS forcing decreases as well, leading to the suppression of the reverse flow of energy.

IV. LOCAL DYNAMIC ENERGY-BASED EDDY-VISCOSITY MODELS

The first step in building localized SGS models is taken by considering eddy-viscosity models where the turbulent viscosity no longer depends on the resolved rate of strain, as in the Smagorinsky approach, but on the SGS kinetic energy. In eddy-viscosity-based models, the unknown SGS stress tensor in Eq. (6) is approximated by

$$\tau_{ij}^*\cong-2\nu_t\overline{S}_{ij}^{>\epsilon}, \tag{12}$$

where $\overline{S}_{ij}^{>\epsilon}=\frac{1}{2}(\partial\overline{u}_i^{>\epsilon}/\partial x_j+\partial\overline{u}_j^{>\epsilon}/\partial x_i)$ is the resolved rate-of-strain tensor and ν_t stands for the turbulent viscosity, which is the model parameter to be expressed in terms of the resolved field. Similarly to what was done in Ref. 14, let us take the square root of k_{SGS} as the velocity scale and the wavelet-filter characteristic width Δ as the length scale for the turbulent eddy-viscosity definition, that is,

$$\nu_t = C_\nu \Delta k_{\mathrm{SGS}}^{1/2}, \tag{13}$$

where C_ν is the dimensionless coefficient to be determined. This way, Eq. (12) is rewritten as

$$\tau_{ij}^* \cong -2C_\nu \Delta k_{\mathrm{SGS}}^{1/2} \overline{S}_{ij}^{>\epsilon}, \tag{14}$$

and the SGS dissipation rate is approximated in terms of the SGS kinetic energy as

$$\Pi \cong C_\nu \Delta k_{\mathrm{SGS}}^{1/2} |\overline{S}^{>\epsilon}|, \tag{15}$$

where $|\overline{S}^{>\epsilon}| = 2\overline{S}_{ij}^{>\epsilon}\overline{S}_{ij}^{>\epsilon}$. Note that the SGS dissipation rate can show both signs, thus allowing for the simulation of local energy backscatter.

Given the eddy-viscosity nature of the model, when solving for the SGS energy, the additional diffusion due to the turbulent viscosity is considered, so that the energy equation (10) is rewritten as

$$\frac{\partial k_{\mathrm{SGS}}}{\partial t} + \overline{u}_j^{>\epsilon}\frac{\partial k_{\mathrm{SGS}}}{\partial x_j} = (\nu + \nu_t)\frac{\partial^2 k_{\mathrm{SGS}}}{\partial x_j \partial x_j} - \epsilon_{\mathrm{SGS}} + \Pi. \tag{16}$$

As mentioned above, in addition to the SGS stress model, the SGS energy dissipation model for ϵ_{SGS} is needed. The latter variable can be modeled, using simple scaling arguments, as

$$\epsilon_{\mathrm{SGS}} = C_\epsilon \frac{k_{\mathrm{SGS}}^{3/2}}{\Delta}, \tag{17}$$

where C_ϵ is the second dimensionless model coefficient (e.g., Refs. 14 and 15) to be determined. Another possibility, not taken here, would be to consider an additional evolution model equation for ϵ_{SGS}, as done, for instance, in Ref. 16.

The wavelet-filtered Navier–Stokes equations (4) and the SGS kinetic energy equation (16) stand for a closed system of coupled equations that is solved with the AWCM methodology briefly described in Sec. II C. In particular, the global thresholding mask for wavelet filtering can be constructed by considering both the velocity and the SGS kinetic energy fields.

In a first lighter version of the model, in order to save computational resources, the model parameters C_ν and C_ϵ are *a priori* prescribed. In particular, the unit value for C_ϵ is fixed, as typically done in LES based on a similar approach. Also, the empirical value $C_\nu = 0.06$ is prescribed for the turbulent viscosity coefficient, as a result of acceptable global matching with the wavelet-filtered DNS solution for the numerical experiments carried out in this work. This one-equation model will be referred to as the localized kinetic-energy-based model (LKM). It is worth stressing that, though the model coefficients are fixed, the LKM procedure is nevertheless "dynamic" in some way as it implicitly takes into account the local energy transfer between the resolved and unresolved motions for the ongoing simulation.

A fully dynamic version of the kinetic-energy-based eddy-viscosity model, with the model coefficients not prescribed but derived from the actual resolved field using the classical Germano dynamic approach,[3] is developed, as illustrated in the following. Let us introduce a secondary test filter with a characteristic filter width $\hat{\Delta} > \Delta$, formally denoting the test-filtered resolved velocity as $\widehat{\overline{u}_i^{>\epsilon}}$. The stress tensor at the test level is given by

$$T_{ij} = \widehat{\overline{u_i u_j}^{>\epsilon}} - \widehat{\overline{u}_i^{>\epsilon}}\,\widehat{\overline{u}_j^{>\epsilon}}, \tag{18}$$

so that filtering [Eq. (5)] at the test level and combining with Eq. (18) results in the following definition for the Leonard stresses:

$$L_{ij} = \widehat{\overline{u}_i^{>\epsilon}\overline{u}_j^{>\epsilon}} - \widehat{\overline{u}_i^{>\epsilon}}\,\widehat{\overline{u}_j^{>\epsilon}} \tag{19}$$

or, equivalently, the popular Germano identity

$$T_{ij} - \hat{\tau}_{ij} = L_{ij}. \tag{20}$$

Once the test filter is given, the Leonard stresses are directly computable on the resolved velocity field and can be exploited to determine the model coefficient with no *a priori* prescriptions. Differently from what was done in Ref. 7, here a low-pass discrete filter is used. Specifically, the discrete low-pass test filter is constructed using the adjacent grid points ensuring the proper filter width and positivity of the filter weights.

The unresolved kinetic energy at the test level, which is referred to as the subtest-scale (STS) kinetic energy, is defined as

$$k_{\mathrm{STS}} = \widehat{\overline{u_i u_i}^{>\epsilon}} - \widehat{\overline{u}_i^{>\epsilon}}\,\widehat{\overline{u}_i^{>\epsilon}}, \tag{21}$$

that is, $k_{\mathrm{STS}} = \frac{1}{2}T_{ii}$. By analogy with Eq. (10), the transport model equation for k_{STS} can be written as

$$\frac{\partial k_{\mathrm{STS}}}{\partial t} + \widehat{\overline{u}_j^{>\epsilon}}\frac{\partial k_{\mathrm{STS}}}{\partial x_j} = (\nu + \nu_t)\frac{\partial^2 k_{\mathrm{STS}}}{\partial x_j \partial x_j} - \epsilon_{\mathrm{STS}} + \Pi_{\mathrm{STS}}, \tag{22}$$

where the STS energy viscous dissipation rate is

$$\epsilon_{\mathrm{STS}} = \nu\left(\widehat{\overline{\frac{\partial u_i}{\partial x_j}\frac{\partial u_i}{\partial x_j}}^{>\epsilon}} - \frac{\partial \widehat{\overline{u}_i^{>\epsilon}}}{\partial x_j}\frac{\partial \widehat{\overline{u}_i^{>\epsilon}}}{\partial x_j}\right), \tag{23}$$

and $\Pi_{\mathrm{STS}} = -T_{ij}^* \widehat{\overline{S}_{ij}^{>\epsilon}}$ stands for the STS energy production, where $\widehat{\overline{S}_{ij}^{>\epsilon}} = \frac{1}{2}(\partial \widehat{\overline{u}_i^{>\epsilon}}/\partial x_j + \partial \widehat{\overline{u}_j^{>\epsilon}}/\partial x_i)$ is the resolved rate-of-strain tensor at the test level. In a similar manner, the kinetic energy that is resolved at the test level can be defined as

$$k_{\mathrm{RTS}} = \widehat{\overline{u}_i^{>\epsilon}\overline{u}_i^{>\epsilon}} - \widehat{\overline{u}_i^{>\epsilon}}\,\widehat{\overline{u}_i^{>\epsilon}} \tag{24}$$

or, equivalently, $k_{\mathrm{RTS}} = \frac{1}{2}L_{ii}$, owing to the Leonard stress definition (19). It is worth noting that, thanks to the positiveness of the employed test filter, the variable k_{RTS} is always nonnegative in the flow field. This way, the Germano identity (20) can be rewritten in terms of the kinetic energy variable as follows:

$$k_{\mathrm{STS}} - \hat{k}_{\mathrm{SGS}} = k_{\mathrm{RTS}}. \tag{25}$$

The above relation allows for the STS kinetic energy to be directly expressed in terms of resolved quantities, which are the velocity and the SGS energy fields. After defining the resolved viscous dissipation at the test level,

$$\epsilon_{\mathrm{RTS}} = \nu\left(\widehat{\frac{\partial \overline{u}_i^{>\epsilon}}{\partial x_j}\frac{\partial \overline{u}_i^{>\epsilon}}{\partial x_j}} - \frac{\widehat{\partial \overline{u}_i^{>\epsilon}}}{\partial x_j}\frac{\widehat{\partial \overline{u}_i^{>\epsilon}}}{\partial x_j}\right), \tag{26}$$

a similar Germano identity relates the energy dissipation rates at test and grid levels,

$$\epsilon_{\mathrm{STS}} - \hat{\epsilon}_{\mathrm{SGS}} = \epsilon_{\mathrm{RTS}}. \tag{27}$$

Again, due to the positiveness of the test filter, the variable ϵ_{RTS} is always non-negative in the flow field. It is worth pointing out that the identity (27) is actually unusable for classical LES formulations since the scale separation acts in the inertial range and the resolved LES field does not contain significant contribution from dissipative scales.[14] Conversely, Eq. (27) can be successfully exploited in the SCALES approach, where also the small-scale energetic structures are resolved.

Different fully dynamic versions of the energy-based eddy-viscosity modeling procedure are presented in the following sections. They are based on either a Bardina-like or a Germano-like approximation for the dynamic determination of the model coefficients C_ν and C_ϵ as space-time functions.

A. Eddy-viscosity modeling

Two different dynamic procedures are proposed to determine the unknown model coefficient for the turbulent eddy viscosity (13).

1. Bardina-like model

By analogy with Eq. (14), let us assume that the Leonard stress can be approximated in terms of the resolved test-scale kinetic energy as follows:

$$L_{ij}^* \cong -2C_\nu \hat{\Delta} k_{\mathrm{RTS}}^{1/2} \widehat{\overline{S}_{ij}^{>\epsilon}}, \tag{28}$$

where, as usual, the star denotes the deviatoric part. The above expression represents a system of five independent equations with the unique unknown C_ν, which can be approximately solved by exploiting a least-squares methodology. This leads to

$$2C_\nu(\boldsymbol{x},t) = \frac{L_{ij}^* \sigma_{ij}}{\sigma_{ln}\sigma_{ln}}, \tag{29}$$

where, for simplifying the notation, the known tensor $\sigma_{ij} = -\alpha\Delta k_{\mathrm{RTS}}^{1/2} \widehat{\overline{S}_{ij}^{>\epsilon}}$ is defined,[17] where $\alpha = \hat{\Delta}/\Delta$ is the test filter to grid ratio.

2. Germano-like model

As an analog of Eq. (14), let us assume that the STS stress can be approximated in terms of the STS kinetic energy as follows:

$$T_{ij}^* \cong -2C_\nu \hat{\Delta} k_{\mathrm{STS}}^{1/2} \widehat{\overline{S}_{ij}^{>\epsilon}}. \tag{30}$$

Therefore, according to the Germano identity (20), combining Eqs. (14) and (30), it holds that

$$-2C_\nu \hat{\Delta} k_{\mathrm{STS}}^{1/2} \widehat{\overline{S}_{ij}^{>\epsilon}} + C_\nu \widehat{\Delta k_{\mathrm{SGS}}^{1/2} \overline{S}_{ij}^{>\epsilon}} = L_{ij}^*, \tag{31}$$

where the coefficient C_ν is assumed to vary slowly in space so that it can be taken out of the test filtering operation. By exploiting the identity (25) and defining

$$M_{ij} = \widehat{k_{\mathrm{SGS}}^{1/2} \overline{S}_{ij}^{>\epsilon}} - \alpha(k_{\mathrm{RTS}} + \hat{k}_{\mathrm{SGS}})^{1/2} \widehat{\overline{S}_{ij}^{>\epsilon}}, \tag{32}$$

a least-squares solution to Eq. (31) leads to the determination of the following local model coefficient:

$$2C_\nu(\boldsymbol{x},t)\Delta = \frac{L_{ij}^* M_{ij}}{M_{ln}M_{ln}}. \tag{33}$$

It is worth stressing that both the present modeling procedures, though based on the same SGS energy-based eddy-viscosity concept, nevertheless, are very different from the dynamic localization model proposed in Ref. 14, where the model coefficient was determined by solving an integral equation in the framework of a constrained variational problem.

B. SGS energy dissipation modeling

Two different dynamic procedures are proposed to determine the unknown model coefficient for the SGS energy dissipation (17).

1. Bardina-like model

According to a Bardina-like approach, by analogy with Eq. (17), let us assume that the resolved test-scale energy dissipation can be approximated as

$$\epsilon_{\mathrm{RTS}} \cong C_\epsilon \frac{k_{\mathrm{RTS}}^{3/2}}{\hat{\Delta}}. \tag{34}$$

The above equation can be solved for the unknown C_ϵ resulting in the following local model coefficient:

$$\frac{C_\epsilon(\boldsymbol{x},t)}{\Delta} = \frac{\alpha\epsilon_{\mathrm{RTS}}}{k_{\mathrm{RTS}}^{3/2}}. \tag{35}$$

2. Germano-like model

According to a Germano-like approach, as an analog of Eq. (17), let us assume that the STS energy dissipation can be approximated as

$$\epsilon_{\mathrm{STS}} \cong C_\epsilon \frac{k_{\mathrm{STS}}^{3/2}}{\hat{\Delta}}. \tag{36}$$

This way, by exploiting the identity (27), after some calculus, the following determination for the SGS energy dissipation coefficient is obtained:

$$\frac{C_\epsilon(\boldsymbol{x},t)}{\Delta} = \frac{\alpha\epsilon_{\mathrm{RTS}}}{(k_{\mathrm{RTS}} + \hat{k}_{\mathrm{SGS}})^{3/2} - \alpha\hat{k}_{\mathrm{SGS}}^{3/2}}. \tag{37}$$

In principle, the above dynamic procedures for determining the model coefficients C_ν and C_ϵ can be adopted independently, leading to four different model combinations. Here, only two different localized dynamic kinetic-energy-

based models (LDKMs) are actually considered for the numerical experiments. The former one (for discussion, LDKM-B) exploits both the Bardina-like dynamic determinations (29) and (35), while the other one (for discussion, LDKM-G) uses both the Germano-like dynamic coefficients (33) and (37).

V. DSM

In this section, a dynamic one-equation non-eddy-viscosity SGS model is developed for the SCALES methodology. The model, recently introduced for LES (e.g., Refs. 16 and 18), is based on the dynamic structure assumption. Namely, it borrows the structure of the unknown SGS stress tensor directly from the resolved Leonard stress (19), without involving the resolved rate-of-strain tensor. The significant similarity between the SGS and the Leonard stresses, which has been observed in real as well as numerical experiments (e.g., Ref. 19), is exploited in the model. Thanks to this similarity, one can consider $\tau_{ij}/\tau_{ll} \cong L_{ij}/L_{hh}$, so that the following approximation holds:

$$\tau_{ij} \cong \frac{k_{\mathrm{SGS}}}{k_{\mathrm{RTS}}} L_{ij}, \tag{38}$$

which corresponds, in particular, to the algebraic form of the model proposed in Ref. 16.

Clearly, the solution of an additional transport equation for k_{SGS} is still an integral part of the modeling procedure. However, due to the non-eddy-viscosity nature of the DSM, the original version (10) is used in this case. According to Eq. (38), the modeled SGS dissipation becomes proportional to k_{SGS},

$$\Pi \cong - \frac{k_{\mathrm{SGS}}}{k_{\mathrm{RTS}}} L_{ij}^{*} \overline{S}_{ij}^{>\epsilon}, \tag{39}$$

and again can show both signs. Note that the present approach does not involve the definition of any model coefficient, while, for the SGS kinetic energy dissipation ϵ_{SGS}, the model (17) can be used together with one of the dynamic procedures discussed in Sec. IV B.

Like for the above eddy-viscosity models, the DSM (38), coupled with the solution of the energy equation (10), provides a positive feedback mechanism that automatically stabilizes the numerical solution. However, according to some authors, the DSM, which is in some ways similar to the classical scale-similarity Bardina model,[20] does not provide sufficient SGS dissipation for LES and therefore should be used as part of a mixed model (e.g., Ref. 17). Nevertheless, as already pointed out in Ref. 16, the pure DSM can be successfully used for decaying isotropic turbulence simulation. This is confirmed by the results of the present study (see Sec. VI).

Finally, let us address some general issues about the use of the auxiliary variable k_{SGS} in SCALES, apart from the particular model implemented. When numerically solving the evolution equation for the SGS kinetic energy by means of the AWCM numerical method, owing to the nonlinearity of the definition (9), additional small scales are created with respect to the solution of the primary variables. Given the adopted coupled wavelet thresholding strategy, discussed in Sec. II B, that automatically leads to an increase in the local grid fineness, with the unavoidable deterioration of the SCALES grid compression. As practically experienced by the authors, one can obtain a field compression comparable to one of the CVS solution (e.g., see Ref. 7), so invalidating the use of the SGS model. To bypass the problem, as already successfully tested for local modeling based on the Lagrangian approach,[8] an artificial diffusion term can be added to the right-hand side of the energy equation, namely, $(\partial/\partial x_j)[\mathcal{D}_k(\partial k_{\mathrm{SGS}}/\partial x_j)]$. To stem the creation of small scales in k_{SGS} field, the artificial diffusion time scale, $\Delta^2/\mathcal{D}_k$, must be smaller than the convection time scale associated with the local strain $|\overline{S}^{>\epsilon}|^{-1}$ that results in fixing $\mathcal{D}_k = \mathcal{C}_k \Delta^2 |\overline{S}^{>\epsilon}|$, where $\mathcal{C}_k$ is a dimensionless parameter of order unity. In practice, for the present numerical experiments, the value $\mathcal{C}_k = 0.1$ has been verified to suffice for the purpose.

Another important aspect that needs to be mentioned is the sensitivity of the SGS energy-based models to the initial value of k_{SGS}. Setting the initial k_{SGS} too high can result in excessive SGS dissipation leading to an incorrect energy evolution. This is particularly dangerous for transient flows such as homogeneous decaying turbulence, while it is negligible for statistically steady turbulent flows such as forced turbulence, as demonstrated by the results discussed in Sec. VI A. A way to make the solution less sensitive to the initial condition is under study and will be the subject of a future work.

TABLE I. Summary of the different localized dynamic kinetic energy SGS models.

Acronym	SGS stress model	SGS kinetic energy dissipation model
LKM	Eddy viscosity, fixed coefficient	Fixed coefficient
LDKM-G	Eddy viscosity, dynamic Germano	Dynamic Germano
LDKM-B	Eddy viscosity, dynamic Bardina	Dynamic Bardina
DSM	Dynamic structure model	Fixed coefficient

VI. NUMERICAL EXPERIMENTS

In this section, the results of the numerical experiments are presented and discussed. The proposed one-equation models, summarized for the sake of clarity in Table I, are evaluated by performing SCALES of incompressible isotropic freely decaying turbulence in a cubic box with periodic boundary conditions. Though these localized models are specifically designed to simulate complex nonhomogeneous turbulent flows, it is nevertheless enlightening to test them for a case in which well known theoretical and experimental results exist. Moreover, decaying turbulence is a challenging example of statistically unsteady flow and is a good test case for *a posteriori* verifying the accuracy of both the SGS stress and the SGS energy dissipation models.

The simulation settings are chosen as follows. The initial velocity field is a realization of a statistically steady turbulent flow at $\mathrm{Re}_{\lambda} \cong 72$ (where λ is the Taylor microscale), as pro-

vided by a fully dealiased pseudospectral DNS solution with 128^3 Fourier modes.[6] The simulation of decaying turbulence is conducted for a temporal range of approximately ten initial eddy-turnover times that corresponds to a final value of $\mathrm{Re}_\lambda \cong 22$. Due to the finite-difference nature of the AWCM solver, the initial resolution has been doubled in each direction in order to keep the DNS spectral energy content intact. In other words, SCALES is run using a maximum resolution corresponding to 256^3 grid points that corresponds to have $j_{\max}=8$ in Eq. (2).

The choice of the thresholding parameter ϵ for wavelet filtering is crucial in the SCALES approach, as it determines the real turbulence resolution. As already mentioned, the amount of SGS dissipation becomes negligible for very small ϵ, with SCALES approaching CVS (Ref. 9) and, for even smaller values, wavelet-based DNS. On the other hand, when the threshold is too large, the adaptive grid is too coarse, too many modes are discarded so that the turbulent energy cascade can no longer be captured. All the results reported in this paper have been obtained using the wavelet thresholding parameter $\epsilon=0.43$ as a compromise between the above mentioned requirements. Furthermore, this allows for a fair comparison with the reference global dynamic model (GDM) solution of Ref. 7, where the same thresholding level was adopted.

As regards the energy equation, the following initial condition has been used for the SGS kinetic energy: $k_{\mathrm{SGS}}(\boldsymbol{x},0)=\beta_k(\langle k^0_{\mathrm{res}}\rangle/\langle k^0_{\mathrm{RTS}}\rangle)k^0_{\mathrm{RTS}}$, where k^0_{res} and k^0_{RTS} are evaluated, according to definitions (7) and (24), on the initial wavelet-filtered DNS field. The coefficient β_k determines the initial ratio between residual and resolved energy that corresponds to the desired turbulence resolution. Based on previous *a priori* studies, it is set for the present experiments to $\beta_k=0.1$.

In Fig. 1, the kinetic energy decay for the different models is illustrated, along with the reference GDM and wavelet-filtered DNS solutions. All the new proposed models capture the energy decay slightly better than the global model. As to the energy spectral distribution, Figs. 2 and 3 show the spectra at two different time instants or, equivalently, two different Re_λ, namely, $\mathrm{Re}_\lambda \cong 46$ ($t=0.08$) and $\mathrm{Re}_\lambda \cong 35$ ($t=0.16$). The localized dynamic SCALES solutions generally show acceptable energy spectra when compared to wavelet-filtered DNS at different times. Note that for the cases where there are no significant wavelet coefficients above level $j=6$, the energy spectra lines stop at wavenumber 32.

Before going on with the discussion of the results, it is worth stressing the fact that modeled solutions showing the right energy decay as well as the correct energy spectra are not sufficient by itself to assess the effectiveness of the modeling procedure. In fact, the AWCM solver used in SCALES allows automatic refinement of the numerical mesh in flow regions where the model does not provide the adequate dissipation. For this reason, a deeper insight must be gained by examining the actual grid compression. As mentioned in Sec. II A, the compression can be defined as the ratio between the number of discarded and total allowable wavelet coefficients (or, equivalently, the same ratio in terms of grid points). In order for the SCALES approach to be successful, the number of grid points actually used during the simulation must be less than that required for a CVS solution of the same problem with no model. Otherwise, the adoption of a SGS model would appear useless, if not inappropriate.

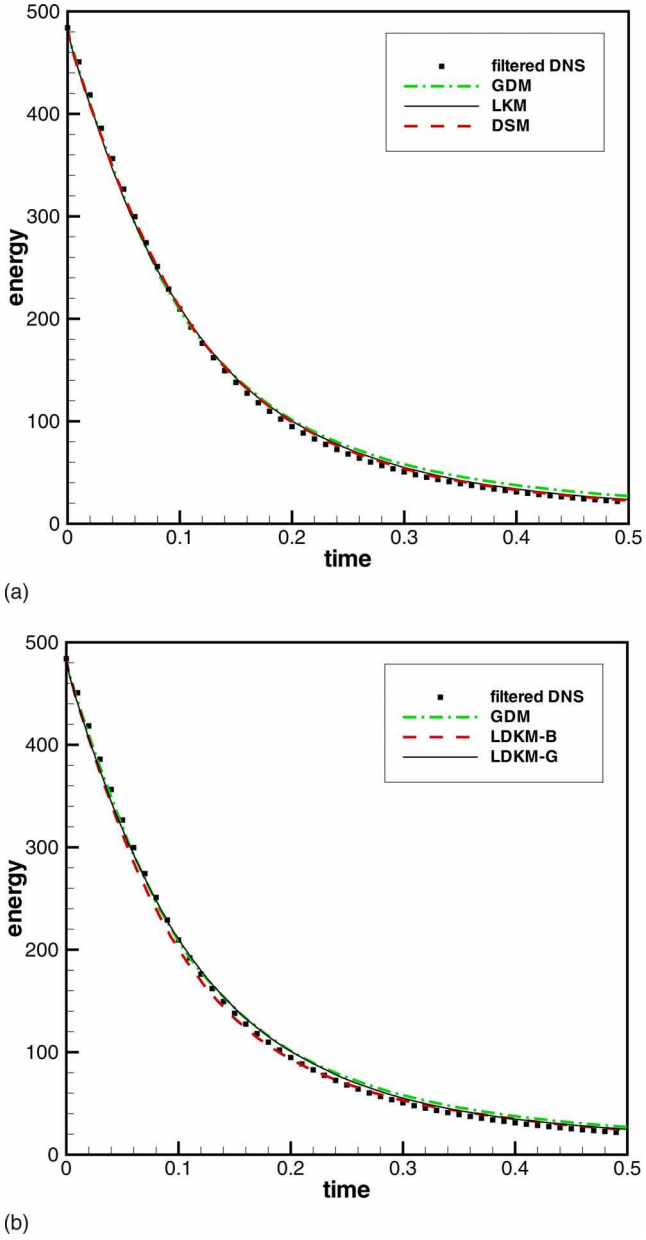

FIG. 1. (Color online) Energy decay: (a) LKM (—) and DSM (- - -); (b) LDKM-B (- - -) and LDKM-G (—). The reference GDM (–·–) and wavelet-filtered DNS (□) solutions are shown for comparison.

The effectiveness of the SGS modeling is first demonstrated by making a comparison with the no-model solution. The latter has been found to be initially underdissipative (see Fig. 7), thus confirming the need for the extra dissipation provided by the SGS model. However, the absence of modeled SGS dissipation results in energy transfer to the small scales, where the energy is dissipated by viscous stresses. Owing to the self-adaptive nature of the numerical method, this process results in increasing the number of resolved modes that causes the solution in practice to evolve toward the DNS approach.

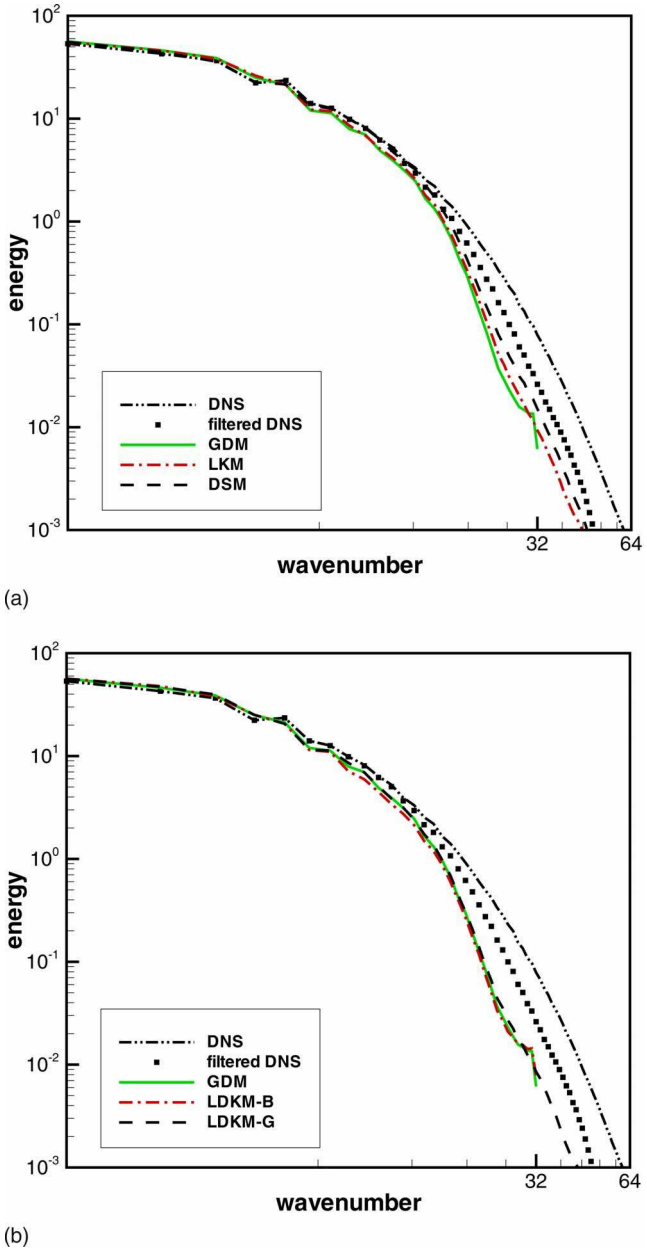

FIG. 2. (Color online) Energy spectra at $t=0.08$: (a) LKM (–·–) and DSM (- - -); (b) LDKM-B (–·–) and LDKM-G (- - -). The reference GDM (—) and wavelet-filtered DNS (□) solutions are shown for comparison, along with the unfiltered DNS (–··–).

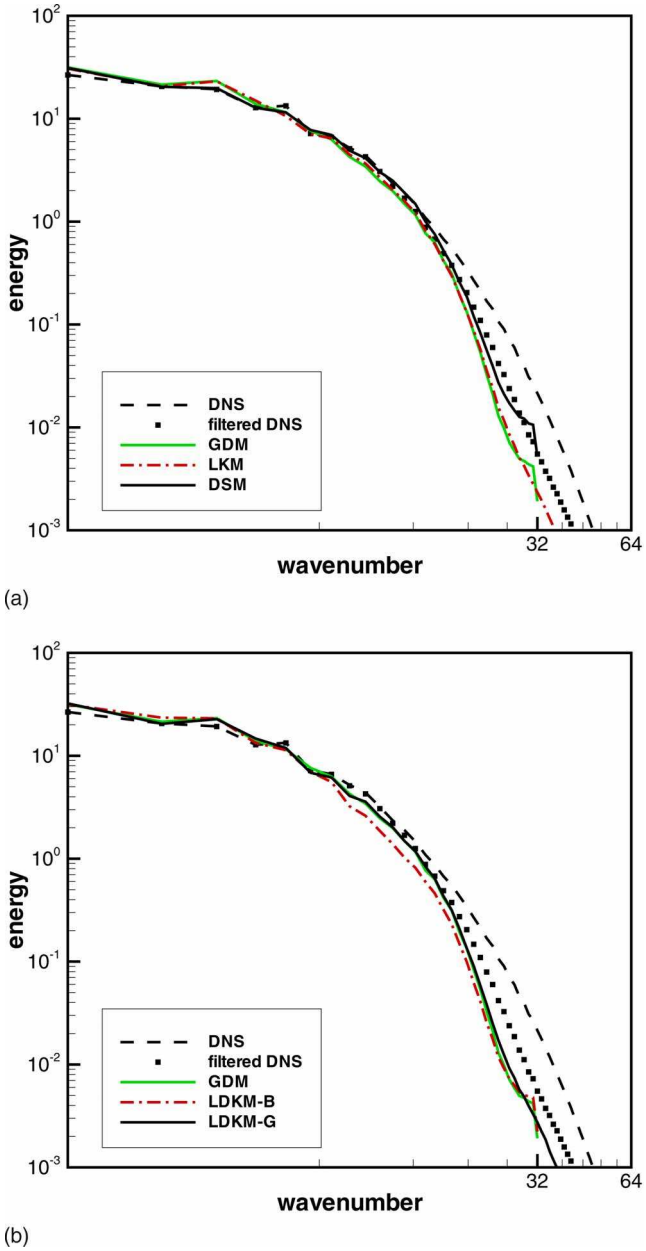

FIG. 3. (Color online) Energy spectra at $t=0.16$: (a) LKM (–·–) and DSM (- - -); (b) LDKM-B (–·–) and LDKM-G (- - -). The reference GDM (—) and wavelet-filtered DNS (□) solutions are shown for comparison, along with the unfiltered DNS (–··–).

As shown in Fig. 4, the gain in terms of compression with respect to the no-model solution is clear. The present grid compression is above 99.5% for all the different proposed models at all time instants, which corresponds to retaining about 1% of the 192^3 modes used for dealiasing by the pseudospectral DNS.[6] The achieved compression is comparable to the reference GDM.[7] The fact that different models show different compression, though using the same relative wavelet thresholding level, is not surprising because the adaptive gridding is closely coupled to the flow physics and, therefore, it is strongly affected by the presence and type of the SGS stress model forcing.

The direct coupling of grid compression with resolved and SGS dissipation can be clearly seen by examining Figs. 4–6. The decrease of SGS dissipation (in the DSM case) results in the decrease of grid compression and the increase of resolved energy dissipation. This reinforces the above discussion about the effectiveness of the model. Also note that, despite the initial similar compression and similar initial level of SGS dissipation, the compression for the GDM is higher. In fact, the nonlocal character of the GDM results in overdissipation at small scales and fewer wavelet coefficients on the finest levels, which ultimately results in the earlier complete removal of the highest level of resolution from the adaptive computational grid, as clearly seen in Figs. 2 and 3. In contrast to the global model, the new models are capable

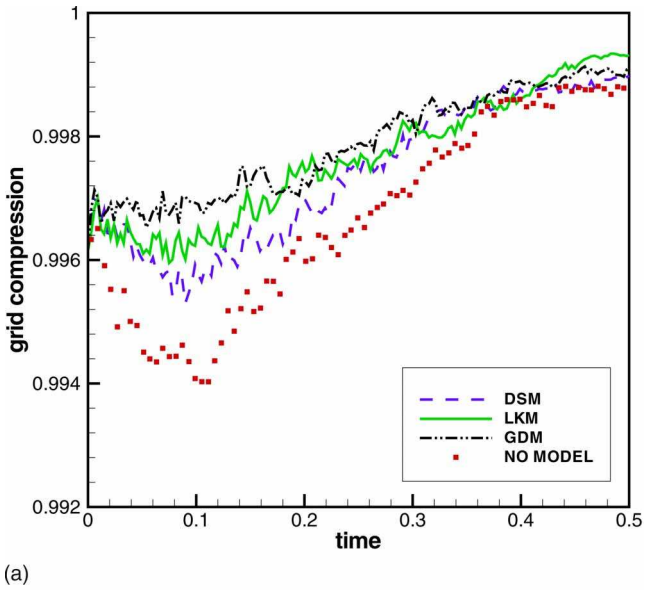

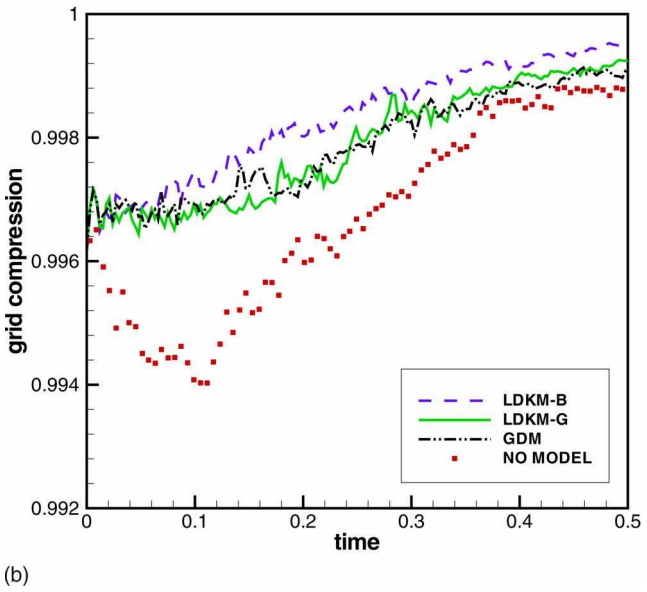

FIG. 4. (Color online) Grid compression: (a) DSM (- - -) and LKM (—); (b) LDKM-B (- - -) and LDKM-G (—). The no-model (□) and GDM (–·–) solutions are shown for comparison.

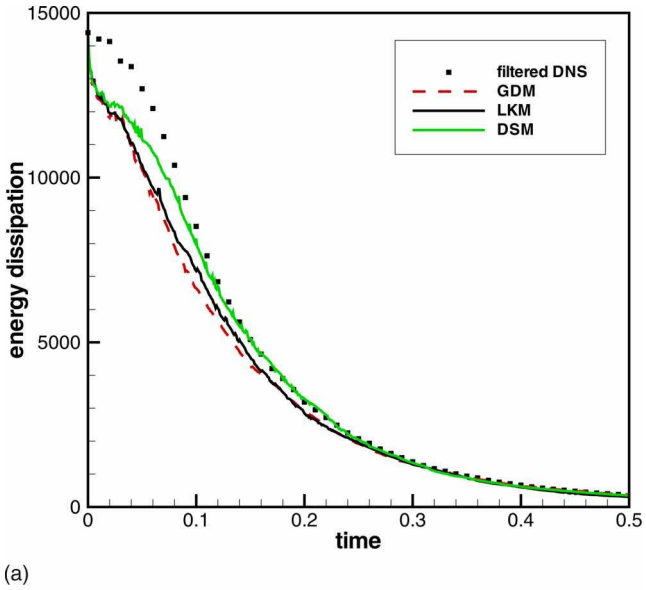

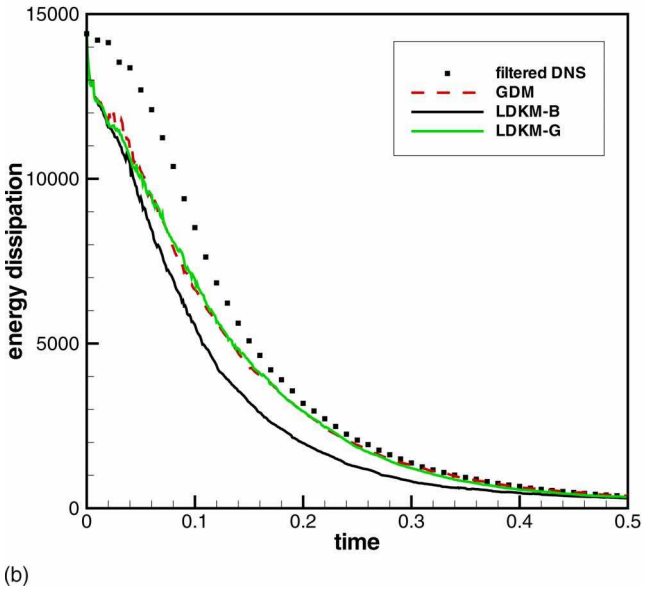

FIG. 5. (Color online) Energy dissipation: (a) LKM (—) and DSM (–·–); (b) LDKM-B (—) and LDKM-G (–·–). The reference GDM (- - -) and wavelet-filtered DNS (□) solutions are shown for comparison.

of capturing the local structure of the flow rather than providing only the mean energy dissipation.

We want to emphasize that, differently from classical LES, the SCALES solution matches the filtered DNS not only in terms of temporal evolution of the total resolved energy (or other global quantities) but also in terms of recovering the DNS energy and enstrophy spectra up to the dissipative wavenumber range. This close match is achieved by using less than 0.5% of the total nonadaptive nodes required for a DNS calculation with the same wavelet solver. To highlight the significance of such an agreement, one can compare the present results (as shown in Figs. 1 and 2) with those corresponding to 64^3 finite-difference nonadaptive LES supplied with either the global dynamic Smagorinsky model (as reported in Ref. 21) or the present energy-based SGS models. Despite the fact that LES solutions use about three times the number of modes, they fail to capture the small-scale features of the flow and the resolved kinetic energy spectrum is noticeably lower than the filtered DNS one for moderate and high wavenumbers. This leads to the underestimation of the energy content of the flow field so that the LES solutions appear overdissipative for the first half of the simulation period, as illustrated in Figs. 7 and 8, where the energy evolution and energy spectra for nonadaptive LES supplied with energy-based models are reported. These differences are more pronounced for the enstrophy spectra, which are illustrated in Fig. 9 (for $t=0.08$). This is even more important since the enstrophy spectra, if properly normalized, coincide with the viscous dissipation spectra, so that the close agreement provided by wavelet-based adaptive LES ensures proper spectral distribution of resolved viscous dissipation.

Finally, it is instructive to discuss the "unexpected," by

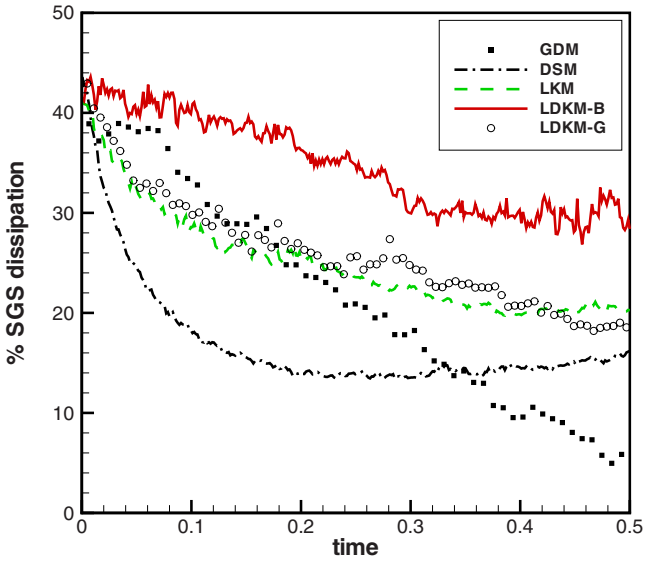

FIG. 6. (Color online) Percentage of SGS dissipation: DSM (–·–), LKM (- - -), LDKM-B (—), and LDKM-G (○) compared to GDM (□).

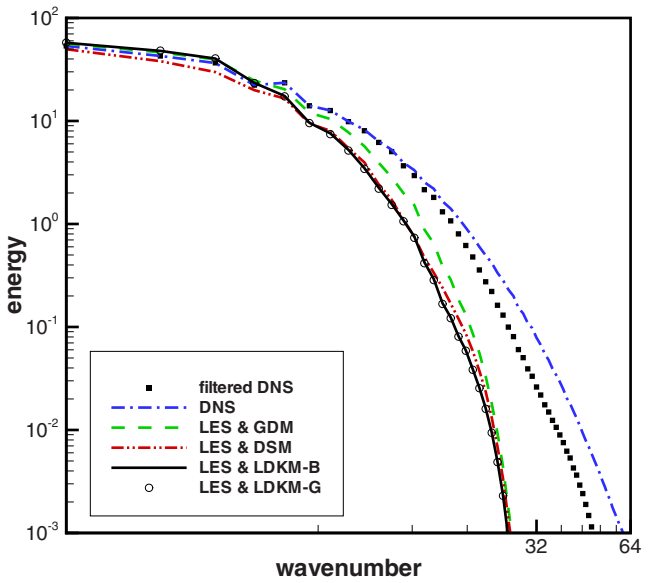

FIG. 8. (Color online) Energy spectra at $t=0.08$ for nonadaptive LES supplied with energy-based models: DSM (–··–), LDKM-B (—), and LDKM-G (○), along with the corresponding GDM (- - -). The wavelet-filtered DNS (□) and unfiltered DNS (–·–) spectra are shown for comparison.

classical LES standards, good performance of the DSM. In fact, in LES formulations, pure similarity models fail in providing the right SGS dissipation, leading to underdissipative solutions, and therefore they require an eddy-viscosity model to be used in conjunction with them. In this work, the capability of the SCALES method to resolve small dissipative scales, at the small additional cost of slightly lower compression, makes it possible to avoid the use of an additional dissipative mechanism as in mixed formulations. Even though the present results are certainly affected by the low Reynolds-number nature of the flow, one can expect a similar good behavior to hold also for higher Reynolds-number simulations. This is one of the objectives of future work on the subject.

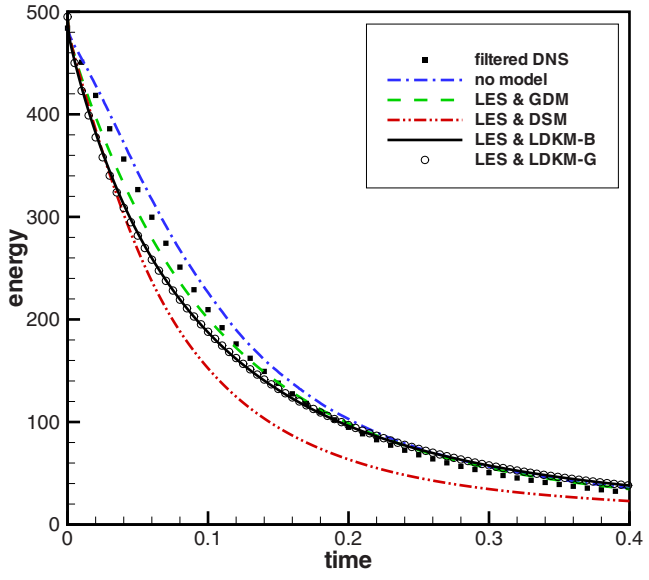

FIG. 7. (Color online) Energy decay for nonadaptive LES supplied with energy-based models: DSM (–··–), LDKM-B (—), and LDKM-G (○), along with the corresponding GDM (- - -). The wavelet-filtered DNS (□) and no-model (–·–) solutions are shown for comparison.

A. Forced turbulence

In order to test the energy-based modeling procedure for a statistically steady flow, let us consider the case in which a forcing term f_i is added at the right-hand side of the momentum equation (4). Namely, following the linear forcing scheme proposed by Lundgren,[22] let the force be proportional to the velocity, $f_i=Q\widetilde{u}_i^{>\epsilon}$, where Q is a constant parameter that can be determined from the energy balance corresponding to the steady state. This way, the solution is continuously supplied with the amount of energy necessary to keep the total resolved energy (statistically) constant in time. In fact, the parameter Q can be showed to be directly linked to the eddy-turnover time of the turbulent velocity field (e.g., Ref. 23). For the present numerical experiments, $Q=6$ is used, which corresponds to have $\tau_{\text{eddy}}=0.056$. The initial velocity field is obtained by wavelet filtering of the fully dealiased pseudospectral 128^3 DNS statistically steady solution with $\text{Re}_\lambda \cong 60$. The simulation is conducted for a temporal range of approximately 100 eddy-turnover times.

The kinetic energy evolution for the LDKM-B solution of linearly forced homogeneous turbulence is illustrated, along with the reference unfiltered pseudospectral DNS, in Fig. 10. The corresponding time-averaged energy spectra are shown in Fig. 11. Once again, it is worth stressing how the wavelet-based solution is able to reproduce to some extent the energy of the small-scale motions. The SCALES solution shows a grid compression that is in average as high as 97%, while the SGS dissipation is of the same order of magnitude as the resolved viscous dissipation. Moreover, by properly redefining the Taylor microscale in terms of the total energy dissipation, resolved viscous dissipation plus SGS dissipa-

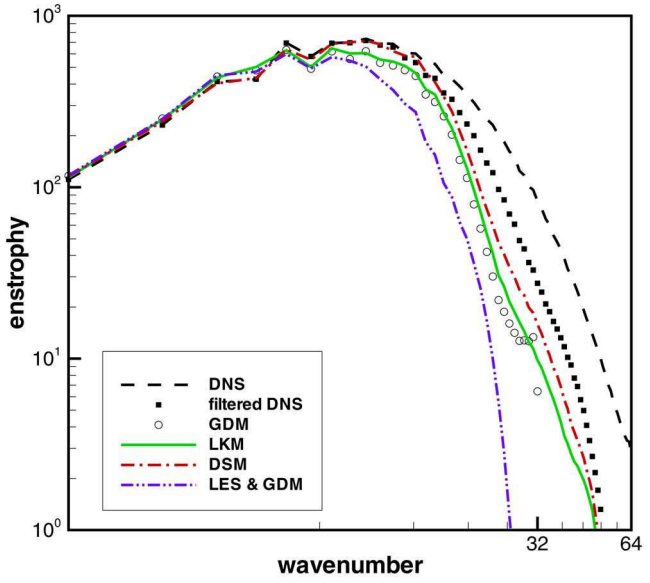

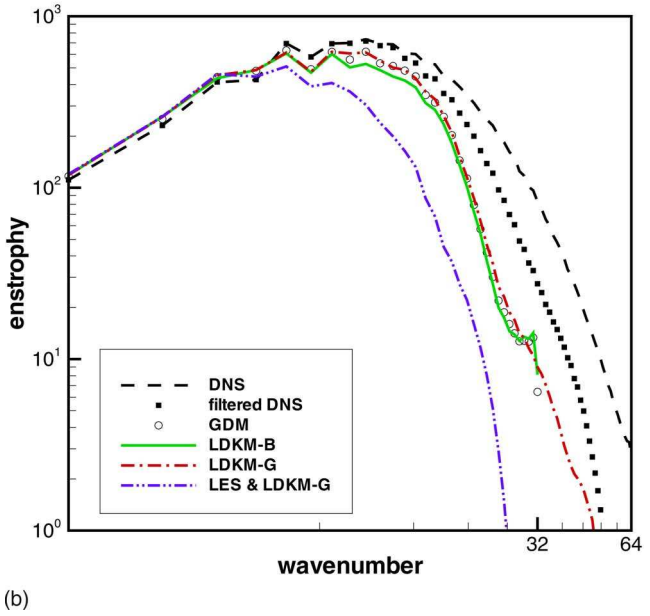

FIG. 9. (Color online) Enstrophy spectra at $t=0.08$: (a) LKM (—), DSM (–·–), and nonadaptive LES supplied with GDM (–···–); (b) LDKM-B (—), LDKM-G (–·–), and nonadaptive LES supplied with LDKM-G (–···–). The reference GDM (○) and wavelet-filtered DNS (□) solutions are shown for comparison, along with the unfiltered DNS (- - -).

tion, the wavelet-based solution provides the same Reynolds number as the reference DNS. These results demonstrate the effectiveness and efficiency of the energy-based SGS model in the forced case.

Finally, to definitely verify the stabilizing action of the built-in feedback mechanism associated with the dynamic energy-based modeling procedure, the following experiment is conducted: the initial SGS kinetic energy content of the flow is artificially altered by multiplying the variable $k_{\mathrm{SGS}}(\boldsymbol{x},0)$ by a factor of either 10^2 or 10^{-2}. This way, the initial SGS energy is either much more or less than the equilibrium value provided by the wavelet-filtered DNS solution. Nevertheless, the LDKM procedure is able to provide a flow

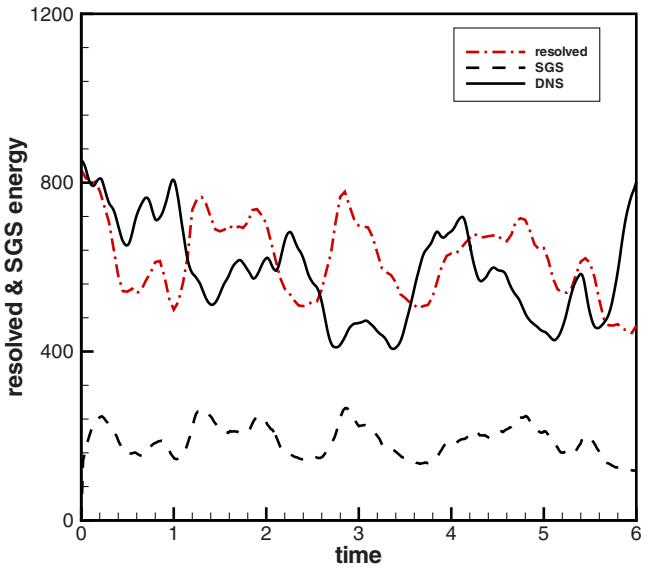

FIG. 10. (Color online) LDKM-B solution of forced turbulence: resolved (–·–) and SGS (- - -) energy, along with the reference DNS solution (—).

evolution that converges after some time toward the unaltered stable solution so that the equilibrium levels are restored. This is clearly illustrated by inspection of Fig. 12, where the evolutions of resolved and SGS energy are reported. This demonstrates that the energy-based method works in practice: solving a subgrid energy transport equation properly represents the energy transfer between resolved and SGS motions, both forward and backscatter.

VII. CONCLUSIONS AND PERSPECTIVES

New localized dynamic models for SCALES that involve an evolution equation for the subgrid kinetic energy are proposed. One of the main advantages of the present formulation is that the equilibrium assumption between pro-

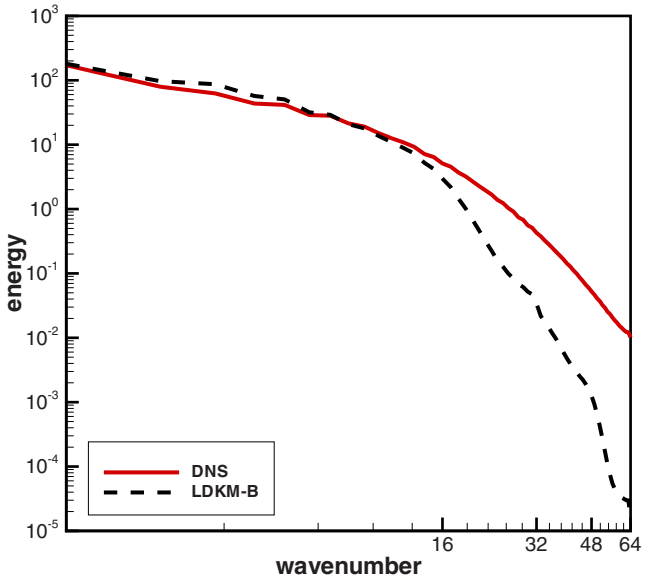

FIG. 11. (Color online) LDKM-B solution of forced turbulence: averaged energy spectrum (- - -) along with the reference DNS (—).

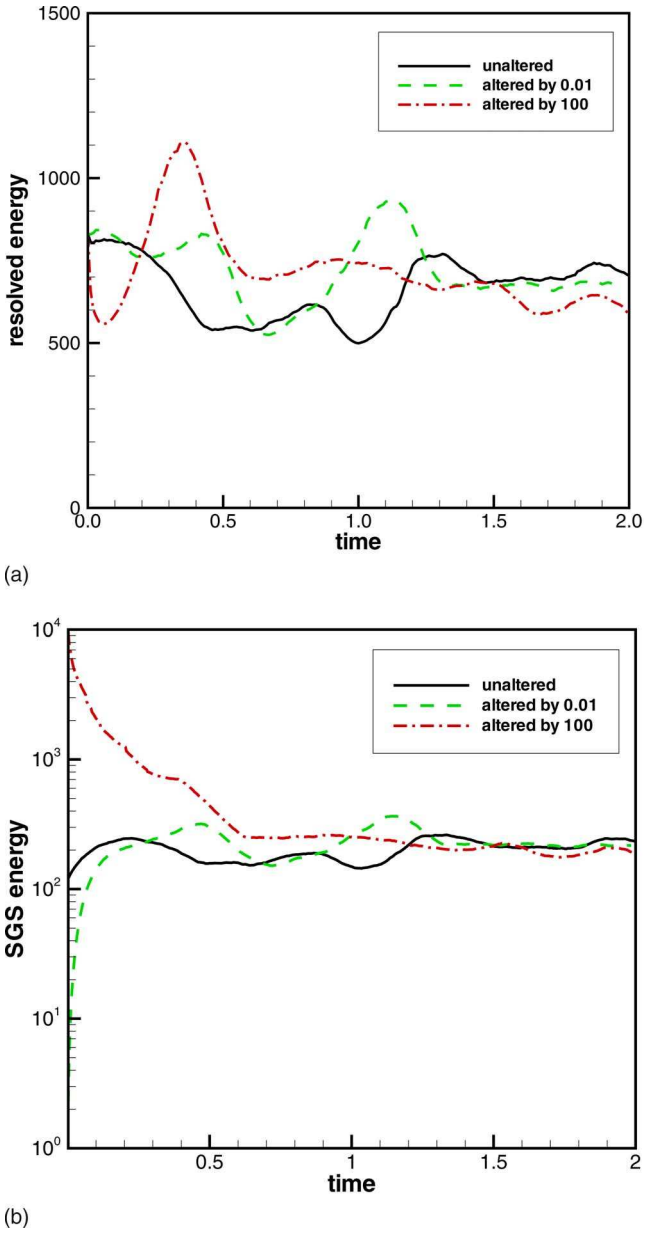

FIG. 12. (Color online) Energy evolutions for LDKM-B solution of forced turbulence with initial SGS energy altered by a factor of either 10^2 (–·–) or 10^{-2} (- - -): (a) resolved and (b) SGS energy are reported along with the unaltered solution (—).

duction and dissipation of SGS energy is not required as in the classical Smagorinsky approach. In contrast, the energy transfer between resolved and residual motions is directly ensured by solving an additional transport model equation for the SGS energy. Some known difficulties, associated with the classical dynamic Germano model, are overcome using these models. Specifically, scaling SGS in terms of the SGS kinetic energy provides a feedback mechanism that makes the numerical simulation stable regardless of whether an eddy-viscosity or non-eddy-viscosity assumption is made. This way, no averaging procedure is needed in practice and the models stay fully localized in space.

The present study demonstrates how the proposed one-equation models work for statistically unsteady flows shedding light on the possible use of the SCALES methodology for complex flow simulation. The energy-based models are assessed in terms of both accuracy and efficiency. In fact, the results match the filtered DNS data at different times with a grid compression comparable if not higher than that achieved with the GDM.

Furthermore, for forced turbulence simulation, it is demonstrated that the dynamic energy-based modeling procedure obtains a stable solution with the level of energy and the energy spectrum comparable to those ones of the corresponding reference spectral DNS. It is verified that the model actually controls backscatter-induced instabilities over long time integration.

As to future work, once a more cost effective implementation is developed, the method will allow for the simulation of complex nonhomogeneous and statistically unsteady flows. For instance, transitional as well as intermittent turbulent flows of engineering interest will be simulated without the need of introducing additional *ad hoc* assumptions for calibrating the SGS model parameters. Also, by explicitly taking care of the residual kinetic energy, the use of one-equation models will allow the numerical simulation of high Reynolds-number flows with reasonable computational grids, which is one of the primary objectives of the SCALES development.

Finally, it is worth stressing that, with the introduction of the SCALES methodology, the incompleteness of classical LES implementations has been partly removed. However, the approach maintains a certain subjectivity due to the prescription of the relative thresholding level for wavelet filtering. A fully adaptive SCALES formulation in which this threshold automatically varies in time based on the instantaneous flow conditions is under study. For instance, as suggested in Ref. 4, the ratio between SGS and resolved kinetic energy can be assumed as a measure of the actual turbulence resolution. Thus, by explicitly involving an evolution equation for the residual kinetic energy, the wavelet thresholding level could be automatically varied in order to maintain the desired level of turbulence resolution for the ongoing simulation.

ACKNOWLEDGMENTS

This work was supported by the Department of Energy (DOE) under Grant No. DE-FG02-05ER25667, the National Science Foundation (NSF) under Grant Nos. EAR-0327269 and ACI-0242457, and the National Aeronautics and Space Administration (NASA) under Grant No. NAG-1-02116. In addition, G.D.S. was partially supported by a grant from Regione Campania (LR 28/5/02 n.5).

[1] J. S. Smagorinsky, "General circulation experiments with the primitive equations," Mon. Weather Rev. **91**, 99 (1963).
[2] J. W. Deardorff, "Three-dimensional numerical study of turbulence in an entraining mixed layer," Boundary-Layer Meteorol. **7**, 199 (1974).
[3] M. Germano, U. Piomelli, P. Moin, and W. Cabot, "A dynamic subgrid-scale eddy-viscosity model," Phys. Fluids A **3**, 1760 (1991).
[4] S. B. Pope, "Ten questions concerning the large-eddy simulation of turbulent flows," New J. Phys. **6**, 1 (2004).
[5] D. E. Goldstein and O. V. Vasilyev, "Stochastic coherent adaptive large eddy simulation method," Phys. Fluids **16**, 2497 (2004).

[6]G. De Stefano, D. E. Goldstein, and O. V. Vasilyev, "On the role of sub-grid scale coherent modes in large eddy simulation," J. Fluid Mech. **525**, 263 (2005).
[7]D. E. Goldstein, O. V. Vasilyev, and N. K.-R. Kevlahan, "CVS and SCALES simulation of 3D isotropic turbulence," J. Turbul. **6**, 1 (2006).
[8]O. V. Vasilyev, G. De Stefano, D. E. Goldstein, and N. K.-R. Kevlahan, "Lagrangian dynamic SGS model for SCALES of isotropic turbulence," J. Turbul. **9**, 1 (2008).
[9]M. Farge, K. Schneider, and N. K.-R. Kevlahan, "Non-Gaussianity and coherent vortex simulation for two-dimensional turbulence using an adaptive orthogonal wavelet basis," Phys. Fluids **11**, 2187 (1999).
[10]M. Farge, K. Schneider, G. Pellegrino, A. A. Wray, and R. S. Rogallo, "Coherent vortex extraction in three-dimensional homogeneous turbulence: Comparison between CVS-wavelet and POD-Fourier decompositions," Phys. Fluids **15**, 2886 (2003).
[11]O. V. Vasilyev, "Solving multi-dimensional evolution problems with localized structures using second generation wavelets," Int. J. Comput. Fluid Dyn. **17**, 151 (2003), special issue on high-resolution methods in computational fluid dynamics.
[12]N. K.-R. Kevlahan and O. V. Vasilyev, "An adaptive wavelet collocation method for fluid-structure interaction at high Reynolds numbers," SIAM J. Sci. Comput. (USA) **26**, 1894 (2005).
[13]O. V. Vasilyev and N. K.-R. Kevlahan, "An adaptive multilevel wavelet collocation method for elliptic problems," J. Comput. Phys. **206**, 412 (2005).
[14]S. Ghosal, T. S. Lund, P. Moin, and K. Akselvoll, "A dynamic localization model for large-eddy simulation of turbulent flows," J. Fluid Mech. **286**, 229 (1995).
[15]U. Schumann, "Subgrid scale model for finite difference simulations of turbulent flows in plane channels and annuli," J. Comput. Phys. **18**, 376 (1975).
[16]E. Pomraning and C. J. Rutland, "Dynamic one-equation nonviscosity large-eddy simulation model," AIAA J. **40**, 689 (2002).
[17]W.-W. Kim and S. Menon, "An unsteady incompressible Navier–Stokes solver for large eddy simulation of turbulent flows," Int. J. Numer. Methods Fluids **31**, 983 (1999).
[18]S. G. Chumakov and C. J. Rutland, "Dynamic structure subgrid-scale models for large eddy simulation," Int. J. Numer. Methods Fluids **47**, 911 (2005).
[19]S. Liu, C. Meneveau, and J. Katz, "On the properties of similarity subgrid-scale models as deduced from measurements in a turbulent jet," J. Fluid Mech. **262**, 83 (1994).
[20]J. Bardina, J. H. Ferziger, and W. C. Reynolds, "Improved turbulence models based on large eddy simulation of homogeneous incompressible turbulence," Thermosciences Division, Mechanical Engineering Department, Stanford University, Report No. TF-19, 1983.
[21]O. V. Vasilyev, D. E. Goldstein, G. De Stefano, D. Bodony, D. You, and L. Shunn, "Assessment of local dynamic subgrid-scale models for stochastic coherent adaptive large eddy simulation," in *Proceedings of the 2006 Summer Program* (Center for Turbulence Research, NASA Ames/Stanford University, Stanford, CA, 2006), pp. 139–150.
[22]T. S. Lundgren, "Linearly forced isotropic turbulence," *Annual Research Briefs* (Center for Turbulence Research, NASA Ames/Stanford University, Stanford, CA, 2003), pp. 461–473.
[23]C. Rosales and C. Meneveau, "Linear forcing in numerical simulations of isotropic turbulence: Physical space implementations and convergence properties," Phys. Fluids **17**, 095106 (2005).